Available online at www.sciencedirect.com
ScienceDirect
Journal of Molecular Catalysis A: Chemical 262 (2007) 98–108
JOURNAL OF MOLECULAR CATALYSIS A: CHEMICAL
www.elsevier.com/locate/molcata

Tungstophosphoric acid supported over zirconia in mesoporous channels of MCM-41 as catalyst in veratrole acetylation

Dhanashri P. Sawant [a], A. Vinu [b], F. Lefebvre [c], S.B. Halligudi [a,*]

[a] *Inorganic Chemistry and Catalysis Division, National Chemical Laboratory, Pune 411008, India*
[b] *International Center for Young Scientists, National Institute for Materials Science, 1-1 Namiki, Tsukuba, Ibaraki 305-0044, Japan*
[c] *Laboratoire de Chimie Organométallique de Surface, CNRS-CPE, Villeurbanne Cedex, France*

Available online 22 August 2006

Abstract

Tungstophosphoric acid (TPA) over zirconia dispersed uniformly in mesoporous silica (MS) channels of MCM-41 and MCM-48 were synthesized and tested for their catalytic activity in veratrole acetylation. Catalysts with different TPA loadings (5–50 wt.%) on 22.4 wt.%ZrO_2/MCM-41 and 15 wt.%TPA on different zirconia loadings (10–70 wt.%)/MCM-41 were prepared and calcined at 1123 K. The physico-chemical characterization of the supported catalysts was done by powder X-ray diffraction (XRD), surface area measurement (BET), scanning electron microscopy (SEM), transmission electron microscopy (TEM), Fourier transformed-infrared (FT-IR) spectroscopy, UV–vis diffuse reflectance spectra, Temperature programmed desorption (TPD) of ammonia, FT-IR pyridine adsorption and ^{31}P cross polarization-magic angle spinning (CP-MAS) NMR spectroscopy. The mesoporous silica supports play an important role in stabilizing catalytically active TPA along with tetragonal phase of zirconia. Among the catalysts, 15 wt.%TPA/22.4 wt.%ZrO_2/MCM-41 calcined at 1123 K was found to have highest acidity and at least four times more active than neat 15 wt.%TPA/ZrO_2 in veratrole acetylation to acetoveratrone by acetic anhydride. Reaction conditions were evaluated with 15 wt.%TPA/22.4 wt.%ZrO_2/MCM-41 calcined at 1123 K to get higher conversion of acetic anhydride to acetoveratrone. The reaction was found to be heterogeneously catalyzed and no contribution from homogeneous (leached) TPA into the medium under the reaction conditions.

Keywords: TPA/ZrO_2; MCM-41; Veratrole; Acetoveratrone; Acetylation

1. Introduction

Friedel-Crafts reactions are among the most versatile methods used for the synthesis of substituted aromatic compounds [1]. Aromatic ketones are either valuable intermediates or end active ingredients in an extensive range of high-value added products, which include pharmaceuticals, agrochemicals, biocides, flavors, fragrances and fine chemicals [2]. Conventional Lewis-acid metal chloride catalysts such as $AlCl_3$, $FeCl_3$, $ZnCl_2$, HF, etc., to synthesize important ketones are useful in a variety of fine chemical industries, which are non-regenerable, used in more than stoichiometric amounts and produce highly corrosive waste streams. Thus, many efforts have been concentrated on finding efficient solid acid catalysts for manufacturing varieties of chemicals through environmentally friendly routes.

Heteropoly acids (HPAs) have been widely used in numerous acid catalyzed reactions due to their strong Brönsted acidity [3–10]. Owing to very low surface area and high solubility in polar solvents, there is a need for the development of supported and heterogeneously active forms of heteropoly acid catalysts. Many reports are available on HPAs supported on metal oxides such as silica [11], active carbon [12], acidic ion-exchange resin [13], titania [14] and zirconia [15–23] Metal oxides that exhibit basic properties like Al_2O_3 and MgO tend to decompose HPAs, causing a significant decrease in their catalytic activities [24–25]. TPA, SO_4^{2-}/ZrO_2 and WO_3/ZrO_2 supported on MCM-41 [26–29] and SBA-15 [30–32] have been reported. Cs-tungstophosphoric acid on mesoporous silica has been synthesized by grafting technique [33] and in nanotubular channels of SBA-15 [34], which further used in acid catalyzed reactions.

Acetoveratrone (3′,4′-dimethoxyacetophenone) is produced from veratrole using mineral acid catalysts, which is used in the synthesis of papaverine (1-(3,4-dimethoxybenzyl)-6,7-dimethoxyisoquinoline), an opium-alkaloid antispasmodic. Acetoveratrone is also synthesized by using hafnium (IV) triflate

* Corresponding author. Tel.: +91 20 25902107; fax: +91 20 25902633.
E-mail address: sb.halligudi@ncl.res.in (S.B. Halligudi).

1381-1169/$ – see front matter © 2006 Elsevier B.V. All rights reserved.
doi:10.1016/j.molcata.2006.08.027

[35], scandium triflate [36] and hafnium triflate as catalysts in presence of lithium perchlorate nitromethane system [37] and carboxylic acid or trisubstituted silyl carboxylates in presence of trifluoromethyl benzoic acid anhydride [38]. Zeolite HY was found to be more active than Hß [39–42] in the above reaction. Cation-exchanged clays were also tested for this reaction [43]. Heteropoly acid supported over hexagonal mesoporous silica (HMS) in presence of 1,2-dichloroethane as a solvent is used for the synthesis of acetoveratrone [44]. However, there is no report on the use of supported heteropoly acid catalysts for acetylation of veratrole in solvent free conditions. TPA/ZrO_2/MS are the new catalyst systems, which provides high surface area, large pore volume, higher acidity and high thermal stability. Hence, it is the purpose of our study to develop such catalyst system, needed for acetylation of veratrole under solvent free conditions.

2. Experimental

2.1. Materials

Cetyltrimethylammonium bromide (CTABr) (Aldrich) and tetraethyl orthosilicate (TEOS) (Aldrich) and sodium silicate (Merck) were used to synthesize mesoporous silica supports. Zirconium oxychloride $ZrOCl_2{\cdot}8H_2O$ (Merck) and 12-tungstophosphoric acid (TPA) were received from Merck. Veratrole and acetic anhydride were purchased from Aldrich and s.d. Fine Chem. Ltd., Mumbai, respectively. All the chemicals were used without further purification. Zeolites with (SiO_2/Al_2O_3 ratio), H–Y (13.5) recovered by calcining NH_4–Y were obtained from Catalysis Pilot Plant (CPP-NCL, Pune). Zn^{2+} exchanged K-10 montmorillonite clay prepared as per literature [43] was used in the above reaction for comparison of the activities in acetylation of veratrole by acetic anhydride. All catalysts were in the powder form and activated prior to their use in the reaction.

2.2. Synthesis

High surface area MCM-41 [45] and MCM-48 [46], i.e. mesoporous silica (MS) supports were synthesized according to the literature procedure. The molar ratio of the synthesis gel composition was $10SiO_2$:$5.4C_{16}H_{33}(CH_3)_3NBr$:$4.24Na_2O$:$1.3H_2SO_4$:$480H_2O$ for MCM-41, while for MCM-48 it was 1 M TEOS:0.25 M Na_2O:0.65 M $C_{16}H_{33}(CH_3)_3NBr$:0.62 M H_2O. The as-synthesized mesoporous samples were calcined in air at 813 K for 8 h. Neat 15 wt.%TPA/ZrO_2 catalyst was prepared by mixing an aqueous solution of required amount of TPA, i.e. 5 ml of distilled water per gram of zirconium oxychloride. The resulting solution was stirred for 2–3 h followed by evaporation to dryness and the resulting solid was dried at 373 K for 12 h, powdered and calcined at 1123 K in air for 4 h.

To study the effect of zirconia (%) loading over MCM-41, pure siliceous MCM-41 was impregnated with an aqueous solution of $ZrOCl_2{\cdot}8H_2O$ with different ZrO_2:MCM-41 weight ratios. The resulting mixture was stirred in a rotary evaporator for 2–3 h followed by evaporation to dryness and dried at 373 K for 12 h and powdered well for further use. These solids were used to prepare catalysts containing known amount of an aqueous solution of TPA (10–12 ml distilled water) per gram of dried ZrO_2/MCM-41 support by impregnation method. Two types of catalysts were prepared wherein zirconia content was varied in the range 10–70 wt.% along with MCM-41 supports with a fixed 15 wt.%TPA loading and calcined at 1123 K in air for 4 h. In another type, catalysts with different TPA loadings (5–50%) were prepared with a predetermined ZrO_2:MCM-41 (22.4 wt.%) ratio, which corresponded to monolayer coverage [47]. For comparison, 22.4 wt.%ZrO_2/MCM-41, 22.4 wt.%ZrO_2/MCM-48, and 3.36 wt.%TPA/MCM-41 were synthesized by following the above procedure. All catalyst materials were calcined at 1123 K in air for 4 h and used in this study.

2.3. Catalyst characterization

Zr, W and P contents in the resulting solids was determined by inductively coupled plasma-optical emission spectroscopy (ICP-OES) and X-ray fluorescence spectrophotometer by sequential X-ray photoelectron spectrometer (XRF), Rigaku 3070 E Model with Rh target. Before ICP-OES analysis, 10 mg of sample is digested with a mixture of 1–2 ml concentrated HF and 5 ml distilled water for 10 min under reflux condition. The solution is then filtered off and the filterate with a known concentration is submitted for further investigation.

The wide reflections at $2\theta \sim 30^\circ$, 50° and 60° characteristics of the ZrO_2-t (tetragonal) phase were detected using X-ray powder diffraction with Cu Kα radiation (Rigaku Model D/MAXIII VC, Japan, $\lambda = 1.5418$ Å). The BET surface area, pore volume and pore size distribution of samples were measured with an Omnisorb 100CX (Coulter, USA) system under liquid N_2 temperature, using N_2 as an adsorbent. Sample is outgassed at 523 K for 2–3 h under 'helium' before subjecting the sample for N_2-adsorption. Formation of ZrO_2-t nanoparticles in the nanotubular channels of calcined 15 wt.%TPA/22.4 wt.%ZrO_2/MS was detected by TEM (JEOL Model 1200 EX instrument operated at an accelerating voltage at 120 kV) with 50 nm magnification. Shimadzu FTIR-8201PC equipment, in diffuse reflectance spectra (DRS) mode and a measuring range of 600–1200 cm^{-1} was used to obtain the FT-IR spectra of solid samples. DRS spectrum for solid samples were recorded in the range of 200–600 nm using Shimadzu UV-2101PC spectrophotometer, fitted with a diffuse reflectance chamber with inner surface of $BaSO_4$.

The state of TPA on the catalyst was elucidated by ^{31}P CP-MAS NMR spectroscopy (Bruker DSX-300 spectrometer) and spectra was recorded at 121.5 MHz with high power decoupling with a Bruker 4 mm probehead. The spinning rate was 10 kHz and the delay between two pulses was varied between 1 and 30 s to ensure that a complete relaxation of the ^{31}P nuclei occurred. The chemical shifts are given relative to external 85% H_3PO_4.

The total amount of acidity of the catalyst was estimated by temperature programmed desorption (TPD) of NH_3 on Micromeritics AutoChem 2910 instrument. It was carried out after 0.1 g of the catalyst sample was dehydrated at 773 K in dry air for 1 h, purged with helium for 0.5 h. The temperature is decreased to 398 K under the flow of helium and then 0.5 ml NH_3 pulses were supplied to the samples until no more uptake

of NH_3 is observed. NH_3 was desorbed in He flow by increasing the temperature to 813 K with a heating rate of 10 °C min^{-1} measuring NH_3 desorbed by TCD.

The nature of acid sites (Brönsted and Lewis) of the catalyst samples with different loadings were characterized by in situ FT-IR spectroscopy with chemisorbed pyridine in drift mode on FTIR-8300 Shimadzu SSU-8000 instrument with 4 cm^{-1} resolution and averaged over 500 scans. These studies were performed by heating pre-calcined powder samples in situ from room temperature to 673 K with heating rate of 5 °C min^{-1} in a flowing stream (40 ml min^{-1}) of pure N_2. The samples were kept at 673 K for 3 h and then cooled to 373 K and then pyridine vapors (20 μl) were introduced under N_2 flow and the IR spectra were recorded at different temperatures up to 673 K. A resolution of 4 cm^{-1} was attained after averaging over 500 scans for all the IR spectra recorded here.

2.4. Catalytic study

Acetylation of veratrole by acetic anhydride was carried out under N_2 atmospheric pressure in a 50 ml round bottom flask equipped with a magnetic stirrer, a reflux condenser, a septum for sample withdrawal and kept in thermostated oil bath. In a typical experiment, 0.09 g catalyst was added to a solution of veratrole 2.61 g (18.89 mmol) and acetic anhydride 0.39 g (3.82 mmol) and the reaction mixture was heated to 353 K with constant stirring for 1 h. Samples withdrawn periodically were analyzed by Shimadzu gas chromatograph fitted with a fused megabore column SE-52, HP-% (cross-linked 5% PhMe silicone), 30 m in length, 0.53 μm film thickness and a FID. The identity of the products was confirmed by GC-MS (Shimadzu QP 5000) and also by comparing with the authentic standard. Conversion of acetic anhydride was determined on its disappearance in the reaction mixture. Before ICP-OES analysis, 10 mg of sample is digested with a mixture of 1–2 ml concentrated HF and 5 ml distilled water for 10 min under reflux condition. The solution is then filtered off and the filterate with a known concentration is subjected for further investigation. Regeneration of the spent catalyst was carried out by separating the catalyst by filteration and by washing the residue with 1,2-dichloromethane (three to four times) followed by drying and calcination at 773 K for 4 h in an air.

3. Results and discussion

Acetylation of veratrole with acetic anhydride catalyzed by 15 wt.%TPA/22.4 wt.%ZrO_2/MCM-41 under reaction conditions studied gave acetoveratrone (3′,4′-dimethoxyacetophenone) as shown in Scheme 1. It is known that the acetylation reaction proceeds through an acylium intermediate H_3CCO^+, generated from the adsorption of the acylating agent onto the Brönsted acidic sites of the catalyst, which adds to aromatic ring via electrophilic substitution to give the acetylated product.

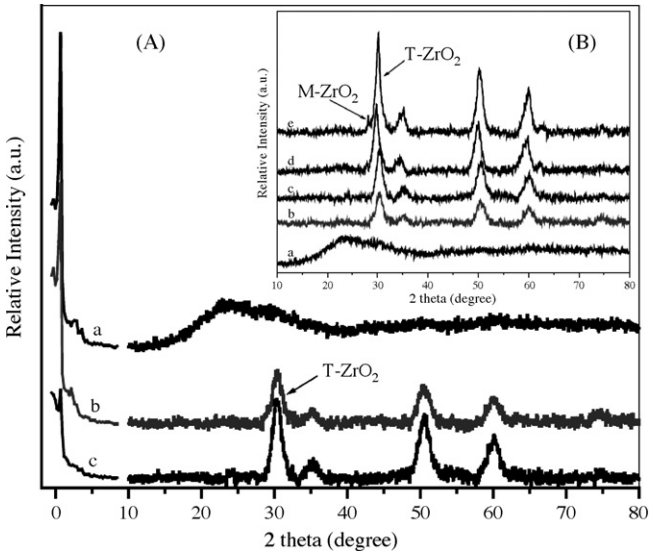

Fig. 1. XRD patterns of (A) (a) 15 wt.%TPA/10 wt.%ZrO_2/MCM-41, (b) 15 wt.%TPA/22.4 wt.%ZrO_2/MCM-41, (c) 15 wt.%TPA/30 wt.%ZrO_2/MCM-41 and (B) wide angle XRD of (a) 15 wt.%TPA/10 wt.%ZrO_2/MCM-41, (b) 15 wt.%TPA/22.4 wt.%ZrO_2/MCM-41, (c) 15 wt.%TPA/30 wt.%ZrO_2/MCM-41, (d) 15 wt.%TPA/50 wt.%ZrO_2/MCM-41, and (e) 15 wt.%TPA/70 wt.%ZrO_2/MCM-41 calcined at 1123 K.

3.1. Characterization of catalyst

The ratio of P:W (1:12) in 15 wt.%TPA/22.4 wt.%ZrO_2/MCM-41 corresponding per Keggin unit was estimated by XRF analysis as (1:12.13) and by ICP-OES analysis as (1:12.07). Fig. 1(A) shows the XRD patterns of 15 wt.%TPA/different wt.%ZrO_2 over MCM-41 and the main diffraction peak corresponding to (1 0 0) reflection of MCM-41 in the mesoporous region was intact up to 22.4 wt.%ZrO_2 loading. At 30 wt.%ZrO_2 loading, intensity of (1 0 0) reflection decreased drastically. Wide-angle XRD patterns showed three well-defined peaks at $2\theta \sim 30°$, 50° and 60°, characteristics of tetragonal ZrO_2 (t-ZrO_2) phase, which could be indexed as (1 1 1), (2 0 2) and (1 3 1), respectively. Furthermore, monoclinic ZrO_2 (m-ZrO_2, $2\theta \sim 28°$) phase also appeared when the ZrO_2/MCM-41 wt.% ratio was higher than 0.5.

Fig. 2(A) and (B) illustrates the XRD patterns of the catalysts with different TPA loadings over 22.4 wt.%ZrO_2/MCM-41. Fig. 2(A) shows that the peaks corresponding to MCM-41

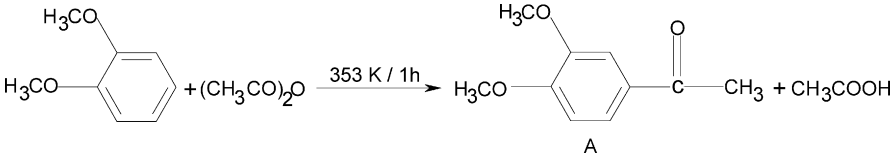

Scheme 1.

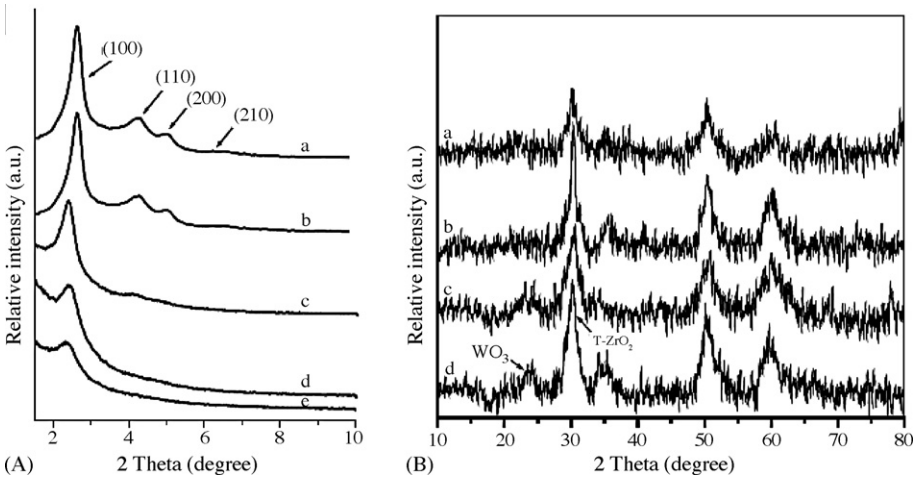

Fig. 2. XRD patterns of (A) (a) MCM-41, (b) 5 wt.%TPA/22.4 wt.%ZrO_2/MCM-41, (c) 15 wt.%TPA/22.4 wt.%ZrO_2/MCM-41, (d) 30 wt.%TPA/22.4 wt.%ZrO_2/MCM-41, and (e) 50 wt.%TPA/22.4 wt.%ZrO_2/MCM-41 and (B) wide angle XRD of (a) 50 wt.%TPA/22.4 wt.%ZrO_2/MCM-41, (b) 30 wt.%TPA/22.4 wt.%ZrO_2/MCM-41, (c) 15 wt.%TPA/22.4 wt.%ZrO_2/MCM-41, and (d) 5 wt.%TPA/22.4 wt.%ZrO_2/MCM-41 calcined at 1123 K.

appeared up to 30 wt.%TPA loading indicating intact mesoporous structure. On further increase in TPA loading, the mesoporous structure of MCM-41 was collapsed. From wide angle XRD, it is seen that up to 15 wt.%TPA loading, TPA/ZrO_2 dispersed uniformly and formed monolayer coverage. With further increase in TPA loading showed a peak corresponding to WO_3 crystallites of decomposed TPA. The powder XRD pattern (Fig. 3) indicated that even after modification, MCM-48 by TPA/ZrO_2, its mesoporosity was intact which exhibited peaks inset as (2 1 1) and (2 2 0). While inset Fig. 3(c) shows zirconia was present only as tetragonal phase with monolayer coverage of TPA over ZrO_2 in MCM-48 channels.

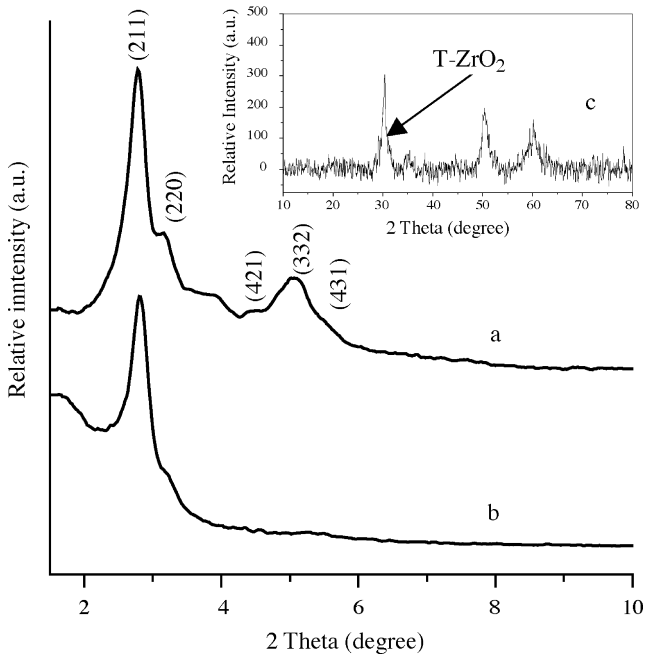

Fig. 3. XRD patterns of (a) MCM-48, (b) 15 wt.%TPA/22.4 wt.%ZrO_2/MCM-48, and (c) (inset figure) wide angle XRD of 15 wt.%TPA/22.4 wt.%ZrO_2/MCM-48.

The surface area, pore volume and pore diameter of the catalysts are presented in Table 1. It is seen (Table 1) that with increase in ZrO_2 loading, marginal decrease in surface area, pore volume and pore diameter was observed as compared to parent MCM-41. It is also seen that a gradual decrease in the above values have been observed with increase in TPA loadings as well. With these observations, it could be presumed that TPA/ZrO_2 was finely dispersed inside mesoporous channels of MCM-41 and MCM-48. The N_2 adsorption-desorption isotherm of 15 wt.%TPA/22.4 wt.%ZrO_2/MCM-41 and 15 wt.%TPA/22.4 wt.%ZrO_2/MCM-48 catalysts are typical of type IV with an unslope but without hysteresis loop at $p/p_0 = 0.2$–0.4 as shown in Fig. 4, just as observed for pure MCM-41 and MCM-48. BJH pore size distribution for 15 wt.%TPA/22.4 wt.%ZrO_2/MCM-41 and 15 wt.%TPA/22.4 wt.%ZrO_2/MCM-48 showed a mean value at 1.97 and 1.72 nm, respectively.

A typical morphology of 15 wt.%TPA/22.4 wt.%ZrO_2/MCM-41 and 15 wt.%TPA/22.4 wt.%ZrO_2/MCM-48 with their parent MCM-41 and MCM-48 were observed through TEM photos as seen in Fig. 5. Transmission electron micrographs of MCM-41 and 15 wt.%TPA/22.4 wt.%ZrO_2/MCM-41 (Fig. 5(a)–(c)) shows a well-defined hexagonal array of unidirectional pore (space group *p6mm*) [48]. The 15 wt.%TPA/22.4 wt.%ZrO_2/MCM-48 sample retains the morphology and cubic-type ordering structure on the (1 1 0) cubic phase similar to those of pure MCM-48 [49] as seen in Fig. 5(d) and (e). TEM analysis also revealed that no obvious extra phases of TPA/ZrO_2 species were present outside the mesoporous channels.

Pure silica exhibited IR bands at 1100 and 806 cm^{-1} and weak shoulder band at 974 cm^{-1} related to surface OH groups. While pure TPA showed characteristic peaks at 1079 cm^{-1} (P–O), 983 cm^{-1} (W=Ot), 893 cm^{-1} (W–Oc–W) and 810 cm^{-1} (W–Oe–W) [50]. The spectra of 15 wt.%TPA/22.4 wt.%ZrO_2/MCM-41, 15 wt.%TPA/22.4 wt.%ZrO_2/MCM-48 and 22.4 wt.%ZrO_2/MCM-41 catalysts are presented in Fig. 6. For TPA/ZrO_2/MS samples, two bands of TPA appeared around 983 and 888 cm^{-1}, while the bands around 1079 and

Table 1
Physicochemical properties of the catalysts and their catalytic activities in acetylation of veratrole at 353 K

Catalyst	S_{BET} (m^2/g)	Pore volume (cm^3/g)	Pore diameter (Å)	Total acidity (mmol g^{-1})	Ac_2O, %Conversion (TOF)[a]	Rate constant ($\times 10^{-5}$) (s^{-1})
MCM-41[b]	1155	0.88	30.5	Nil	Nil	Nil
22.4 wt.%ZrO_2/MCM-41	589	0.38	27.7	0.24	20.5	6.4
15 wt.%TPA/10 wt.%ZrO_2/MCM-41	573	0.33	23.2	0.26	28.4(0.09)	9.3
15 wt.%TPA/22.4 wt.%ZrO_2/MCM-41	516	0.28	19.7	0.33	43.9(0.15)	16.1
15 wt.%TPA/30 wt.%ZrO_2/MCM-41	491	0.24	18.7	0.26	31.7(0.11)	10.6
15 wt.%TPA/50 wt.%ZrO_2/MCM-41	479	0.20	17.8	0.18	10.6(0.04)	3.1
15 wt.%TPA/70 wt.%ZrO_2/MCM-41	402	0.13	15.8	0.15	5.1(0.02)	1.5
5 wt.%TPA/22.4 wt.%ZrO_2/MCM-41	533	0.32	21.7	0.27	32.4(0.32)	10.9
30 wt.%TPA/22.4 wt.%ZrO_2/MCM-41	499	0.22	17.9	0.24	30.5(0.05)	10.1
50 wt.%TPA/22.4 wt.%ZrO_2/MCM-41	481	0.20	17.2	0.19	19.2(0.02)	5.9
MCM-48[b]	1096	0.71	26.1	Nil	Nil	Nil
22.4 wt.%ZrO_2/MCM-48	612	0.62	24.8	0.10	11.1	3.3
15 wt.%TPA/22.4 wt.%ZrO_2/MCM-48	540	0.22	17.2	0.25	27.1(0.09)	8.8
15 wt.%TPA/ZrO_2	11	–	–	0.02	10.9(0.01)	3.2
3.36 wt.%TPA/MCM-41	479	0.19	27.1	0.18	17.5(0.06)	5.3

[a] TOF is calculated by considering three protons per Keggin unit (mol $mol_{H^+}^{-1}$ s^{-1}), *Conditions*: temperature = 353 K; veratrole/Ac_2O molar ratio = 5; catalyst wt. = 0.09 g (3 wt.% of total reaction mixture); time = 1 h.
[b] Except these entries all other catalysts were calcined at 1123 K in air.

810 cm^{-1} overlapped with the strong bands of SiO_2. The spectra of ZrO_2 exhibit a wide band in the range 400–700 cm^{-1} extending up to 1150 cm^{-1} [51]. For samples containing lower TPA loading showed bands with low intensity as compared to bulk TPA spectra, which was due to masking of bands by wide bands of support.

In case of the TPA/ZrO_2 modified mesoporous silica, i.e. MCM-41 and MCM-48 samples, the zirconia and $PW_{12}O_{40}^{3-}$ anion are the detectable species present. The UV–vis spectra of zirconia showed a band at 275 nm [52], while heteropoly acid showed a band at 265 nm for TPA [51]. TPA modified samples showed only one band, as ZrO_2 band was overlapped with strong band of TPA (Fig. 7). Due to the oxygen–metal charge-transfer, the tungstophosphate anion $[PW_{12}O_{40}]^{3-}$ species showed TPA characteristic band at 263–265 nm (Fig. 7) in both 15 wt.%TPA/22.4 wt.%ZrO_2/MCM-41 and 15 wt.%TPA/22.4 wt.%ZrO_2/MCM-48 catalysts samples.

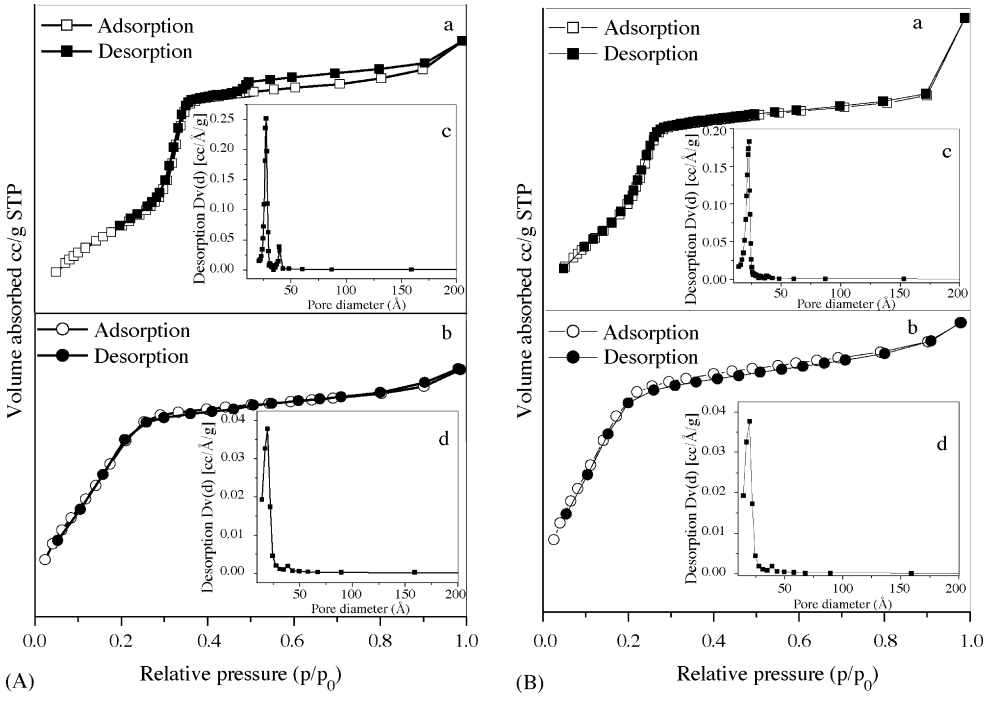

Fig. 4. BET isotherm (A) (a) MCM-41, (b) 15 wt.%TPA/22.4 wt.%ZrO_2/MCM-41, (B) (a) MCM-48, (b) 15 wt.%TPA/22.4 wt.%ZrO_2/MCM-48 and pore size distribution (insight figure), (c) MCM-41, (d) 15 wt.%TPA/22.4 wt.%ZrO_2/MCM-41, (B) (c) MCM-48, and (d) 15 wt.%TPA/22.4 wt.%ZrO_2/MCM-48.

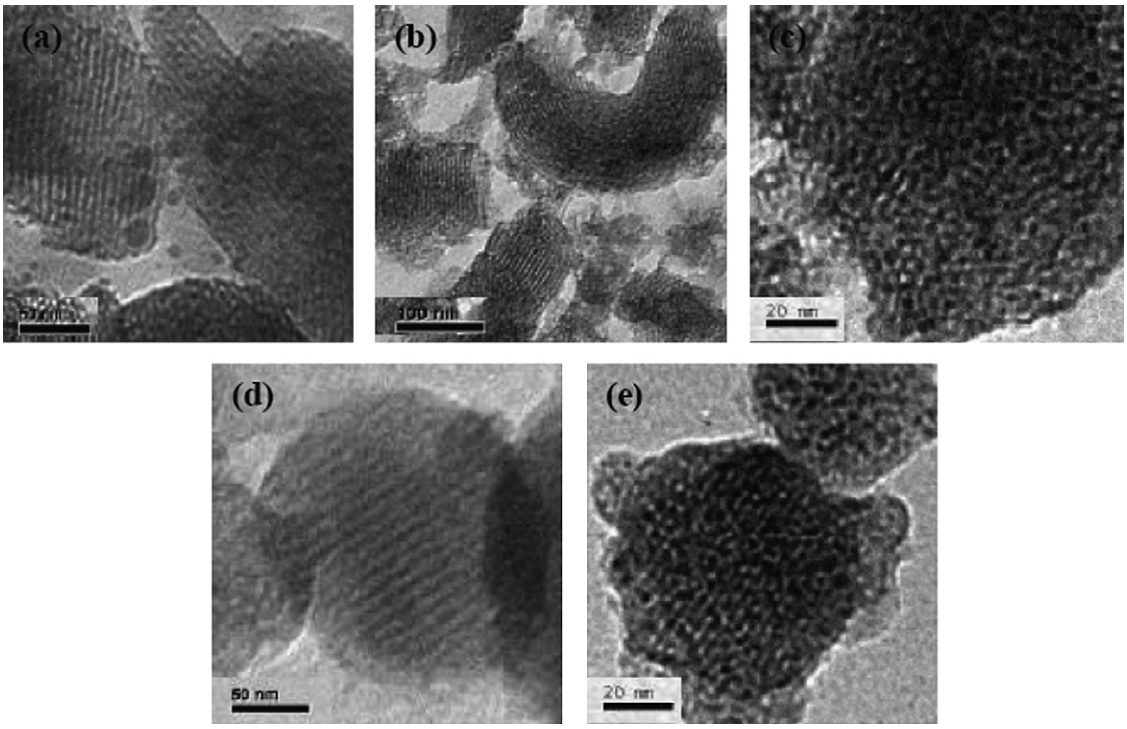

Fig. 5. TEM of (a) MCM-41, (b) and (c) 15 wt.%TPA/22.4 wt.%ZrO_2/MCM-41, (d) MCM-48, and (e) 15 wt.%TPA/22.4 wt.%ZrO_2/MCM-48.

^{31}P CP-MAS NMR spectra for different loadings of TPA shown in Fig. 8 are consistent with XRD observations. Neat TPA shows ^{31}P peak at −12 ppm indicating intact Keggin structure according to literature [53]. Cross-polarization technique has been used because of the low concentration of 'P' in the catalyst systems since TPA/ZrO_2 was embedded inside the mesoporous channels. Hence, very broad spectrum with noisy signal was observed with all the catalysts, where the peak with maximum height was considered as major signal (Fig. 8). It was found that up to 15 wt.%TPA loading, peak at −12.2 ppm was observed as a major one. But on further increase in TPA loading, i.e. for 30 wt.%TPA, it showed two peaks 50–50% peak at −12.2 and −24.8 ppm indicated that TPA decomposed partially into WO_3 crystallites. At 50 wt.%TPA, a new peak appeared at −30 ppm,

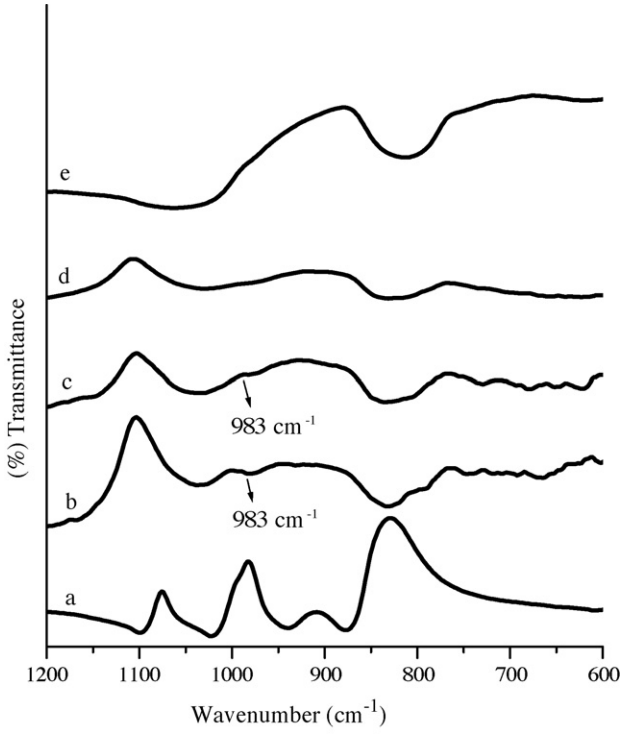

Fig. 6. FT-IR DRS spectra of (a) pure TPA, (b) 15 wt.%TPA/22.4 wt.%ZrO_2/MCM-41, (c) 15 wt.%TPA/22.4 wt.%ZrO_2/MCM-48, (d) 22.4 wt.%ZrO_2/MCM-41, and (e) pure silica calcined at 1123 K.

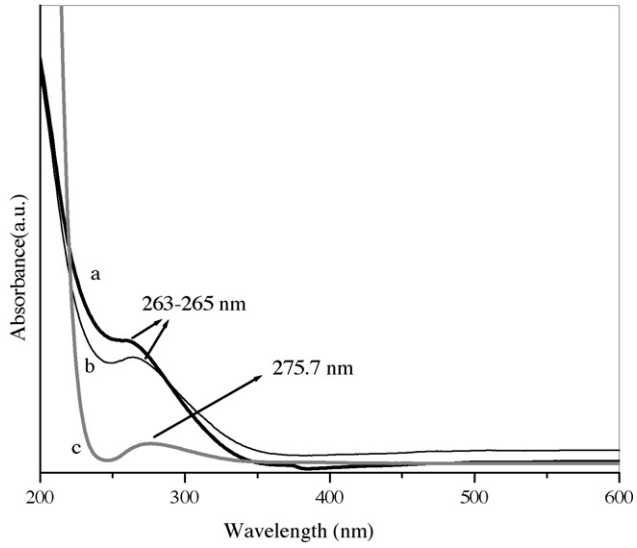

Fig. 7. UV–vis spectra of (a) 15 wt.%TPA/22.4 wt.%ZrO_2/MCM-41, (b) 15 wt.%TPA/22.4 wt.%ZrO_2/MCM-48 calcined at 1123 K, and (c) 22.4 wt.%ZrO_2/MCM-41 calcined at 1123 K.

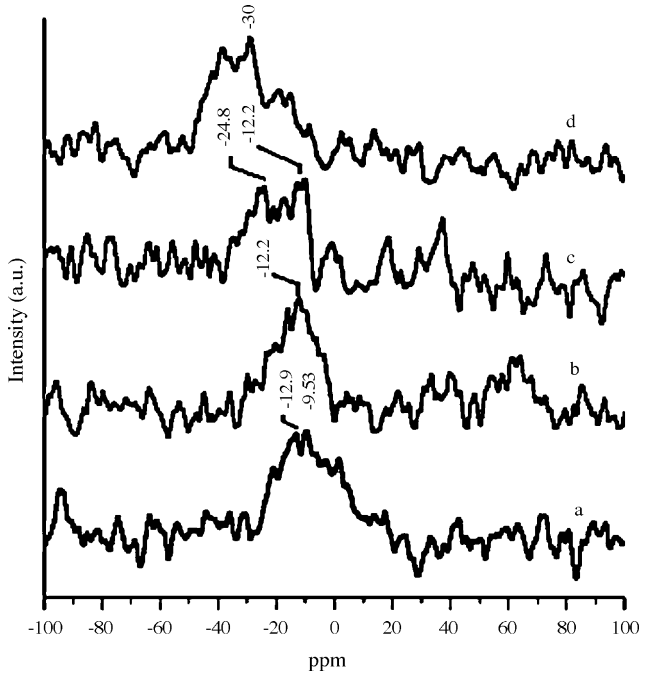

Fig. 8. ^{31}P CP-MAS NMR spectra of (a) 5 wt.%TPA/22.4 wt.%ZrO_2/MCM-41, (b) 15 wt.%TPA/22.4 wt.%ZrO_2/MCM-41, (c) 30 wt.%TPA/22.4 wt.%ZrO_2/MCM-41, and (d) 50 wt.%TPA/22.4 wt.%ZrO_2/MCM-41 calcined at 1123 K.

typical of P–O–P linkages [54], which was associated with phosphorous oxide a by-product of decomposed TPA. These peak positions corresponded to the center of the maximum of the broad peaks. The broad line at −12 ppm is probably related to species formed by linking the Keggin unit to zirconia support. Indeed, the first part of the interaction between TPA and zirconia will be a protonation of surface hydroxyl groups of zirconia, leading to $(\equiv Zr\text{–}OH_2)_n^+[H_{3-n}W_{12}PO_{40}]^{n-3}$ species [10]. Upon heating water will be removed, leading to a direct linkage between the polyanion (which has probably retained a structure similar to that of Keggin ion) and the support. Since our system deals with high temperature (1123 K), so extensive dehydroxylation of TPA is possible to give above species. When the polyanion decomposes, a new signal appears at −30 ppm. As the support is heterogeneous, a distribution of surface species will be obtained. Since TPA/ZrO_2 dispersed uniformly in the MCM-41 channels, instead of sharp peak like bulk TPA, line broadening has been observed in our system. From literature Ref. [55], it is to be noted that the broadening and lowfield shift of ^{31}P NMR peak upon thermal dehydration is consistent with reported studies [56–59]. This is consistent with the fact that P was geometrically at the center of the Keggin anion, i.e. far away from the proton, and that the Keggin anion remained intact, even though some local distortions has occurred.

The temperature-programmed desorption of ammonia (NH_3-TPD) was performed to determine the total amount of acidity of the catalysts. TPD profiles of the 15 wt.%TPA with different wt.% of ZrO_2 over MCM-41 and different TPA loadings over 22.4 wt.%ZrO_2/MCM-41 are shown in Fig. 9(A) and (B), respectively. All samples showed a broad desorption pattern indicating the surface acid strength is widely distributed. While, Table 1 compares the total acidity of TPA/ZrO_2 with different supports including unsupported catalysts. Among these, 15 wt.%TPA/22.4 wt.%ZrO_2/MCM-41 was found to have the highest acidity and thereby highest catalytic activity in acetylation of veratrole by acetic anhydride. The NH_3-TPD data for different TPA (%) loaded catalysts suggested that the total acidity of the catalysts increased up to 15 wt.%TPA loading and decreased with further increase.

Brönsted and Lewis acidity of the catalysts were distinguished by the technique of pyridine adsorption in situ FT-IR spectroscopy and represented in terms of B/L ratio as shown in Fig. 10. The Brönsted/Lewis (B/L) site ratio was calculated from the IR absorbance intensities [60] of bands at 1539 cm^{-1} (B) and 1442 cm^{-1} (L) of 15 wt.%TPA/22.4 wt.%ZrO_2/MCM-41 catalyst calcined at 1123 K and plotted against ZrO_2 (wt.%) and TPA (wt.%) loading as shown in Fig. 10(A) and (B), respectively. It was found that with increase in ZrO_2 content up to 22.4 wt.%, B/L ratio increased and on further increase in ZrO_2 it decreased. As reported [47], the threshold value for monolayer dispersion of ZrO_2 over MCM-41 is 22.4%, which was determined according to the method reported earlier [61]. XPS

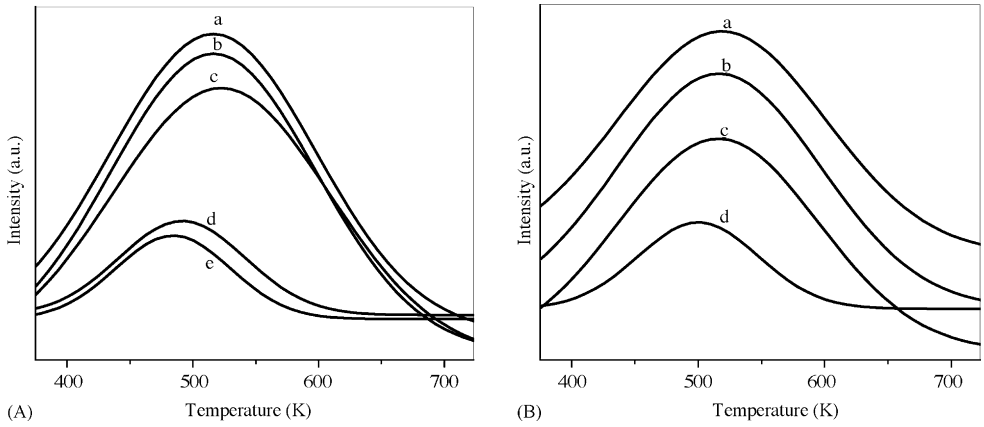

Fig. 9. NH_3-TPD of (A) (a) 15 wt.%TPA/10 wt.%ZrO_2/MCM-41, (b) 15 wt.%TPA/22.4 wt.%ZrO_2/MCM-41,(c) 15 wt.%TPA/30 wt.%ZrO_2/MCM-41, (d) 15 wt.%TPA/50 wt.%ZrO_2/MCM-41, (e) 15 wt.%TPA/70 wt.%ZrO_2/MCM-41 and (B) TPD of NH_3 of (a) 5 wt.%TPA/22.4 wt.%ZrO_2/MCM-41, (b) 15 wt.%TPA/22.4 wt.%ZrO_2/MCM-41, (c) 30 wt.%TPA/22.4 wt.%ZrO_2/MCM-41, and (d) 50 wt.% 15 wt.%TPA/22.4 wt.%ZrO_2/MCM-41 calcined at 1123 K.

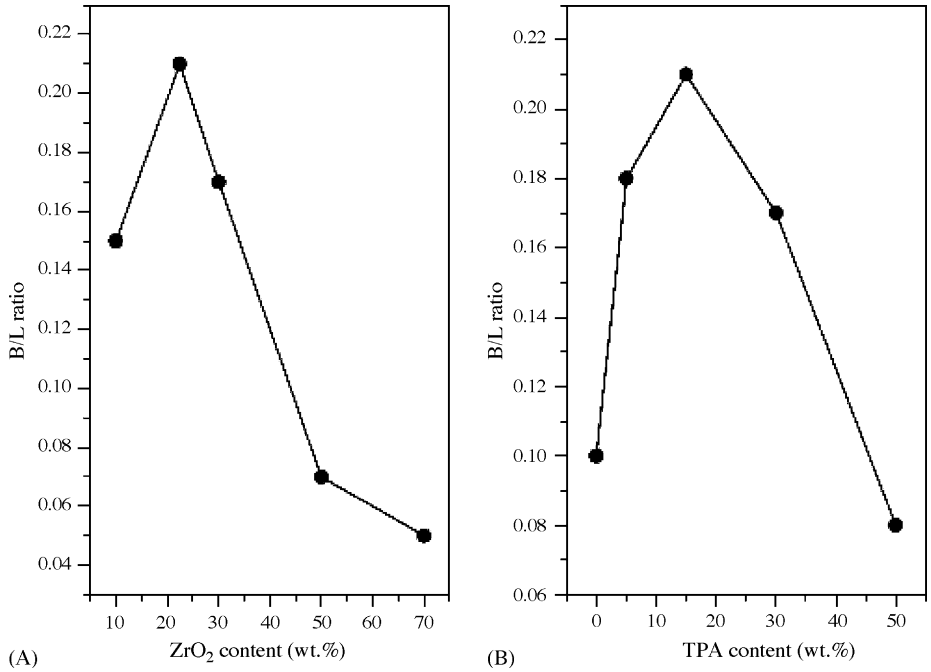

Fig. 10. (A) B/L ratio vs. ZrO_2 content (wt.%) for 15 wt.%TPA/different wt.%ZrO_2/MCM-41 and (B) B/L ratio vs. $H_3PW_{12}O_{40}$ content (wt.%) for different wt.%TPA/22.4 wt.%ZrO_2/MCM-41 calcined at 1123 K.

analysis has been used to investigate the interaction between the guest (ZrO_2) and the host (MCM-41) and was found that ZrO_2 was more likely to interact with MCM-41 by hydrogen bonds involving Si–O–H groups of the MCM-41 with zirconium atoms in ZrO_2. Due to such interaction at monolayer coverage free hydrogen is available from MCM-41 support. While below and above 22.4 wt.%ZrO_2 loading, this interaction was not that predominant due to less ZrO_2 content and also due to multilayer formation in both the mesoporous supports. Similarly, B/L ratio increased with TPA (wt.%) loading up to 15 wt.% and on further increase it decreased. Thus, the sample with 15 wt.%TPA/22.4 wt.%ZrO_2/MCM-41 has the highest acidity, which was due to the monolayer coverage of TPA on ZrO_2 finely dispersed in mesopores of MCM-41. The decrease in B/L ratio and the loss in catalytic activity was due to the decomposition of TPA, which exceeds monolayer coverage at higher TPA loading. The genesis of Brönsted acidity of 15 wt.%TPA/22.4 wt.%ZrO_2/MCM-41 calcined at 1123 K could be explained as, during calcination dehydroxylation of support takes place and in this process interaction of TPA with support would be partially weakened to give free H^+ ions (Brönsted acid sites). Assuming that some TPA protons react with (OH) groups in hydrated zirconia, it would be reasonable to expect that some terminal W=O bonds of TPA might react with partially dehydroxylated $(Zr(–O)_3)^+$ species to form anchored TPA species, e.g. the formation of Zr–O–W bonds. These TPA species would exert an electron withdrawing effect on surface Zr^{4+} cations, making them to behave as strong Lewis acid sites. Keeping in view of all the above facts, we hypothesize that the interaction between TPA and zirconia might be weakened till monolayer coverage (15 wt.% and 1123 K) so that TPA protons are free for reactions to proceed and thereby increasing Brönsted acidity and the total acidity (due to zirconia Lewis acidity increases). While on further increase in TPA loading, might be due to multilayer formation, bulk properties of TPA would be more predominant, causing destruction of TPA to give WO_3 crystallites (partially proved by NMR). The interaction between TPA and zirconia within the allowed phase transformation was responsible for the high acidity.

3.2. Catalytic activity

Acetylation of veratrole by Ac_2O was conducted using different TPA loaded (5–50 wt.%) catalysts to know the effect of TPA loadings on the conversion of Ac_2O and the results are presented in Table 1. Also, turnover frequencies (TOF) and rate constants have been given for the catalysts with different TPA (%), ZrO_2 (%) loadings and as well as for different supports (Table 1). It is seen that MCM-41 is better than MCM-48 support. As, 15 wt.%TPA/22.4 wt.%ZrO_2/MCM-48 has large surface area with less pore volume and pore diameter as compared to 15 wt.%TPA/22.4 wt.%ZrO_2/MCM-41 showed less activity and this could be due to the difference in their pore structures and preferred blocking of pores in case of MCM-48. MCM-41 has a hexagonal array of unidirectional pores (space group *p6mm*), while MCM-48 has cubic pore system (space group *Ia3d*). In addition to this, MCM-48 material possess a bicontinuous structure centered on the gyroid minimal surface that divided available pore space into two non-intersecting subvolumes. Hence, TPA/ZrO_2 might get dispersed in MCM-41 channels more uniformly as compared to MCM-48. From Table 1 it shows that 15 wt.%TPA/22.4 wt.%ZrO_2/MCM-41 shows highest Ac_2O (%) conversion and maximum rate constant as compared to other catalyst systems. Similarly,

22.4 wt.%ZrO_2 gave maximum Ac_2O conversion among different ZrO_2 (%) loaded catalysts. However, the neat 15 wt.%TPA/ZrO_2 gave poor catalytic activity in acetylation of veratrole with a conversion of Ac_2O (10.9%), which is at least four times less than 15 wt.%TPA/22.4 wt.%ZrO_2/MCM-41 calcined at 1123 K under the same reaction conditions. While 3.36 wt.%TPA/ZrO_2 shows 2.5 times less catalytic activity as compared to 15 wt.%TPA/22.4 wt.%ZrO_2/MCM-41. The presence of TPA has significant effect on the catalytic activities. 15 wt.%TPA loaded on 22.4 wt.%ZrO_2/MCM-41 has shown two-fold increase in catalytic activity as compared to 22.4 wt.%ZrO_2/MCM-41 (Table 1). So, we could conclude that in case of composite material, there was an influence of zirconia on the acidity function of TPA and visa versa, which enhanced the catalytic activity due to fine and uniform dispersion of TPA/ZrO_2 together inside large surface area mesoporous silica support. TPA was characterized mainly by Brönsted-type acidity [62], while weakly acidic oxide, i.e. ZrO_2 comprised mainly Lewis-type acid sites [63]. Accordingly, the strongly acidic properties of TPA/ZrO_2 could be attributed to electron-withdrawing effects similar to those ascribed to Zr-bonded sulfate groups [64].

The catalytic activities of H-Y and Zn (II)-exchanged clay catalysts were evaluated in the acetylation of veratrole with acetic anhydride under identical reaction conditions for comparison with the catalytic activity of 15 wt.%TPA/22.4 wt.%ZrO_2/MCM-41 catalyst. The total acidity (mmol/g) and activities expressed in terms of acetic anhydride (Ac_2O) conversion (wt.%) are presented in Table 2. Among the catalysts, H-Y shows comparable catalytic activity with 15 wt.%TPA/22.4 wt.%ZrO_2/MCM-41 due to highest acidity with large pores tri-dimensional zeolite network with supercages. For zeolite, the number of active protons was taken to be equivalent to the Al content [65]. Zn^{2+}-exchanged clay showed poorest TOF (which is expressed per active metal center, i.e. Zn^{2+}) under these reaction conditions, which may be due to the diffusion limitations. But, 15 wt.%TPA/22.4 wt.%ZrO_2/MCM-41 catalyst calcined at 1123 K, shows highest catalytic activity in terms of TOF as 0.15 s^{-1}, with three accessible H^+ per Keggin anion [66] was chosen for further investigations on its catalytic performance in the veratrole acetylation with acetic anhydride.

Here, initial rates w.r.t. conversion of acetic anhydride for different TPA (%) loaded over 22.4 wt.%ZrO_2/MCM-41 catalysts are shown in Fig. 11(A). It is seen that initial rates (expressed in mol min^{-1}) increased with increase in TPA loading up to 15 wt.% and decreased with further increase. Among the catalysts, 15 wt.%TPA/22.4 wt.%ZrO_2/MCM-41 has the highest acidity and hence gave the highest activity.

The effect of catalyst concentration on the conversion of Ac_2O in veratrole acetylation was studied with 15 wt.%TPA/22.4 wt.%ZrO_2/MCM-41 calcined at 1123 K by varying catalyst concentration from 1 to 5 (wt.%) of total reaction mixture. Conversion of Ac_2O increased from 20.8 to 56.7% with increase in catalyst concentration as shown in Fig. 11(B).

The effect of veratrole to acetic anhydride mole ratio over Ac_2O conversion was studied with 15 wt.%TPA/22.4 wt.%ZrO_2/MCM-41 catalyst calcined at 1123 K by varying veratrole/Ac_2O molar ratio in the range 1–9, by keeping other conditions same as shown in Fig. 11(C). The conversion of Ac_2O increased from 25.6 to 62.9% with increase in veratrole/Ac_2O molar ratio up to 9.

The effect of temperature on conversion of Ac_2O was studied in the temperature range 333–373 K and the results are shown in Fig. 11(D). The turn over number (TON) and conversion of Ac_2O increased substantially from 24.9 to 63.7 with increase in temperature.

The rate data for the acetylation of veratrole by Ac_2O in excess of veratrole over 15 wt.%TPA/22.4 wt.%ZrO_2/MCM-41 catalysts could be fitted well to a pseudo-first order rate law. Hence, the standard equations for a first-order series reaction $C_A/C_{Ao} = e^{-k_1 t}$ has been used for the determination of rate constant, where C_{Ao} and C_A are the concentration of Ac_2O at initial time and at time t, respectively. The rate constants calculated for different catalysts are presented in Table 1.

At one particular temperature, first-order rate constants were calculated at different reaction time and then the constant values of 'k_1' showed that the acetylation of veratrole is a first-order reaction. Energy of activation of the reaction was evaluated graphically. The activation energy (E_a) was obtained from an Arrhenius plot (Fig. 12). A linear plot with negative slope equivalent to (E_a/R), which gave an activation energy of 7.89 k cal mol^{-1}.

In order to check the leaching of TPA into the reaction mixture in the course of the reaction, the reaction of acetylation of veratrole with Ac_2O was carried out for 2 h under optimized reaction conditions using fresh 15 wt.%TPA/22.4 wt.%ZrO_2/MCM-41 catalyst calcined at 1123 K. The reaction was stopped after 1h and catalyst was separated by filtration and then the hot filtrate was stirred further for 1 h under same reaction conditions. It was found that in the absence of the catalyst, there was no further increase in the conversion of Ac_2O, which indicated the complete absence of leaching of TPA into the reaction mixture. For testing leaching of TPA after reaction, hot filtrate (separated from catalyst) is checked for the presence of tungsten (W) and phosphorus (P) by inductively coupled plasma-optical emission spectroscopy (ICP-OES, Perkin Elmer-Emission Spectrometer

Table 2
Acetylation of veratrole with acetic anhydride: a comparison between mesoporous with zeolite and clay catalyst

Catalyst	Total acidity (mmol g^{-1})	Ac_2O conversion (mol%)	TOF (mol $mol^{-1}_{H^+ \text{ or } Zn^{2+}}$ s^{-1})
H–Y	2.25	40.0	0.064
Zn^{2+}-montmorillonite K-10 clay	0.67	20.3	0.0039
15 wt.%TPA/22.4 wt.%ZrO_2/SBA-15	0.33	43.9	0.15

Conditions: temperature = 353 K; veratrole/Ac_2O molar ratio = 5; catalyst wt. = 0.09 g (3 wt.% of total reaction mixture); time = 1 h.

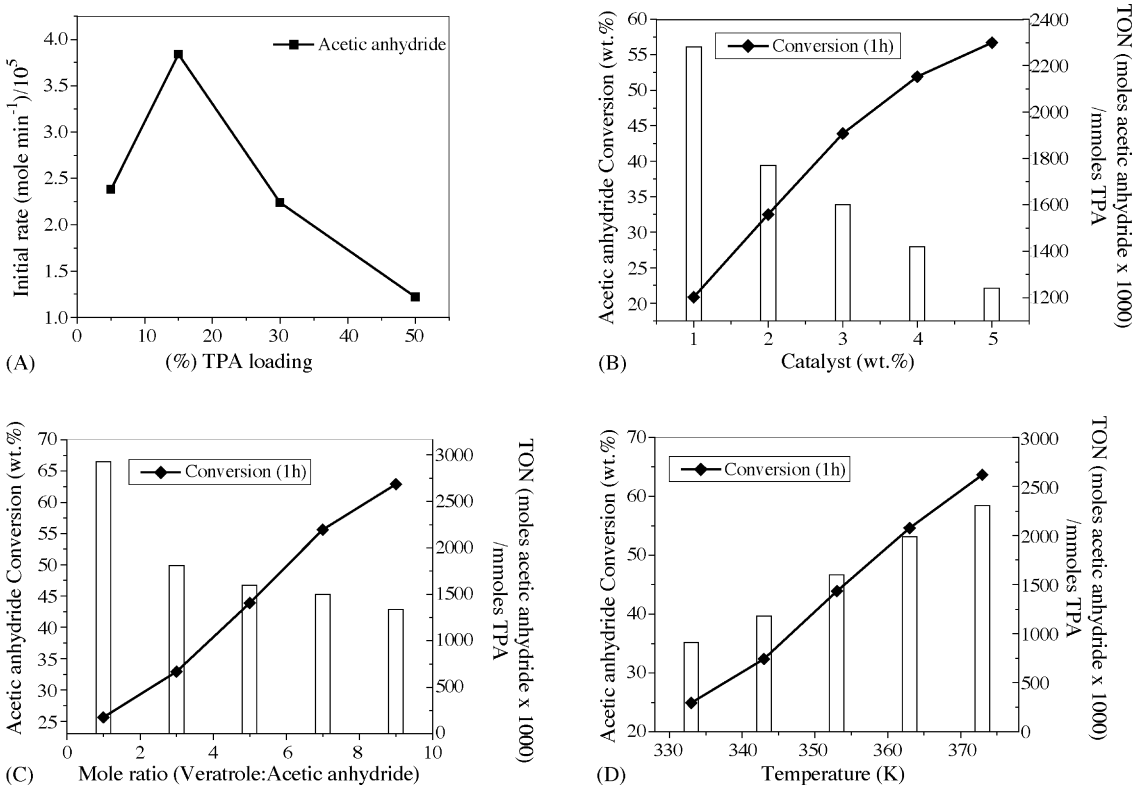

Fig. 11. (A) Initial rate vs. different TPA (%) loading over 22.4 wt.%ZrO_2/MCM-41 calcined at 1123 K. *Conditions*: temperature = 353 K; veratrole/Ac_2O molar ratio = 5; catalyst wt.% = 0.09 g (3 wt.% of total reaction mixture); time = 20 min. (B) Effect of catalyst weight on veratrole acetylation. *Conditions*: temperature = 353 K; veratrole/Ac_2O molar ratio = 5; time = 1 h. (C) Effect of molar ratio on veratrole acetylation. *Conditions*: temperature = 353 K; catalyst wt.% = 0.09 g (3 wt.% of total reaction mixture); time = 1 h. (D) Effect of reaction temperature on veratrole acetylation. *Conditions*: veratrole/Ac_2O molar ratio = 5; catalyst wt.% = 0.09 g (3 wt.% of total reaction mixture); time = 1 h.

Plasma-1000) and it showed the complete absence of both the elements in the filtrate. This observation confirmed that the reaction was catalyzed heterogeneously. The catalyst was regenerated by filtration and then residue was washed three to four times with 1,2-dichloromethane and then dried and calcined at 773 K for 4 h in an air. The data on the catalytic activity of regenerated catalysts in two cycles is presented in Table 3. It is seen that even after second recycle, there was no appreciable loss in the catalytic activity.

Table 3
Recycling of catalysts in acetylation of veratrole with acetic anhydride

Cycle	Ac_2O conversion (wt.%)	Acetoveratrone selectivity (%)	TON
Fresh	43.9	100	1596
Ist	43.6	100	1584
IInd	43.0	100	1566

Conditions: temperature = 353 K; veratrole/Ac_2O molar ratio = 5; catalyst wt. = 0.09 g (3 wt.% of total reaction mixture); time = 1 h; TON (turnover number) = (mole acetic anhydride converted/mmol TPA) × 1000.

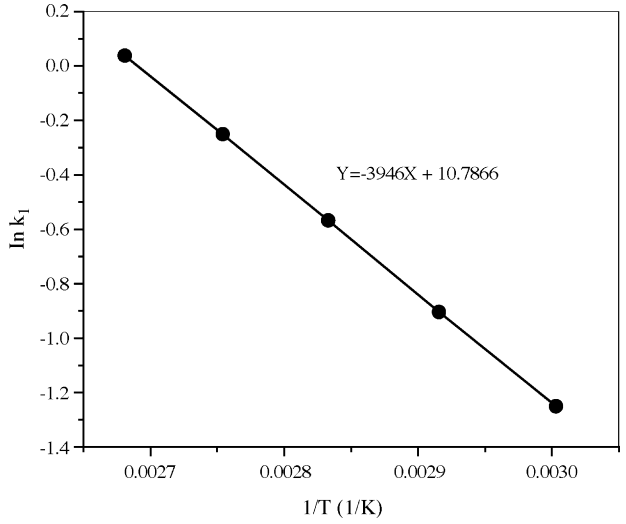

Fig. 12. Arrhenius plot of $\ln k_1$ vs. $1/T$.

4. Conclusions

Acetylation of veratrole with Ac_2O was carried out over 15 wt.%TPA/22.4 wt.%ZrO_2/MCM-41 catalyst calcined at 1123 K in liquid phase conditions under N_2 atmosphere. The catalyst was fully characterized and the stability of TPA on the support has been proved satisfactorily. The 15 wt.%TPA/22.4 wt.%ZrO_2/MCM-41 catalyst gave highest catalytic activity at 353 K with veratrole:Ac_2O molar ratio 5 and 3 wt.% catalyst concentration (of the total reaction mixture) with a maximum conversion of acetic anhydride (43.9%) and 100% selectivity for acetoveratrone (3′,4′-dimethoxyacetophenone).

The rate constant including the activation energy for intrinsic kinetics on the surfaces have been evaluated. The above catalyst was recyclable, cost effective and environmental friendly and could be used in similar reactions.

Acknowledgements

This work was supported financially by DST, New Delhi, under SERC Scheme. Dhanashri P. Sawant acknowledges CSIR, New Delhi, for research fellowship.

References

[1] G.A. Olah, Friedel-Crafts and related reactions, vol.1–4, Wiley–Interscience, New York, 1963/1964.
[2] J.I. Kroschwitz, M. Howe-Grant, Encyclopedia of Chemical Technology, vol. 2, 4th ed., Wiley–Interscience, New York, 1991, p. 213.
[3] L. Marosi, G. Cox, A. Tenten, H. Hibst, J. Catal. 194 (2000) 140.
[4] I.V. Kozhevnikov, Catalysts for Fine chemical synthesis-Catalysis by Polyoxometalates, vol. 2, Wiley–Interscience, Liverpool, UK, 2002.
[5] I.V. Kozhevnikov, Chem. Rev. 98 (1998) 171.
[6] N. Misono, M. Misono, Chem. Rev. 98 (1998) 199.
[7] T. Okuhara, Chem. Rev. 102 (2002) 3641.
[8] T. Okuhara, N. Misono, M. Misono, Adv. Catal. 41 (1996) 113.
[9] T. Okuhara, C. Hu, M. Hashimoto, M. Misono, Bull. Chem. Soc., Jpn. 67 (1994) 1186.
[10] Y. Wu, X. Ye, X. Yang, X. Wang, W. Chu, Y. Hu, Ind. Eng. Chem. Res. 35 (1996) 2546.
[11] Y. Izumi, R. Hasebe, K. Urabe, J. Catal. 84 (1983) 402.
[12] M.A. Schwegler, H. Van Bekkum, N.A. De Munck, Appl. Catal. A-Gen. 74 (1991) 191.
[13] T. Baba, Y. Ono, Appl. Catal. A-Gen. 144 (1996) 59.
[14] J.C. Edwards, C.Y. Thiel, B. Benac, J.F. Knifton, Catal. Lett. 51 (1998) 77.
[15] E. López-Salinas, J.G. Hernández-Cortéz, I. Schifter, E. Torres-García, J. Navarrete, A. Gutiérrez-Carrillo, T. López, P.P. Lottici, D. Bersani, Appl. Catal. A-Gen. 193 (2000) 215–225.
[16] B.M. Devassy, S.B. Halligudi, S.G. Hegde, A.B. Halgeri, F. Lefebvre, Chem. Commun. 10 (2002) 1074.
[17] D.P. Sawant, A. Vinu, N.E. Jacob, F. Lefebvre, S.B. Halligudi, J. Catal. 235 (2005) 341.
[18] D.P. Sawant, S.B. Halligudi, J. Mol. Catal. A: Chem. 237 (2005) 137.
[19] D.P. Sawant, B.M. Devassy, S.B. Halligudi, J. Mol. Catal. A: Chem. 217 (2004) 211.
[20] B.M. Devassy, F. Lefebvre, S.B. Halligudi, J. Catal. 231 (2005) 1.
[21] B.M. Devassy, S.B. Halligudi, J. Catal. 236 (2005) 313.
[22] B.M. Devassy, G.V. Shanbhag, F. Lefebvre, W. Böhringer, J. Fletcher, S.B. Halligudi, J. Mol. Catal. A: Chem. 230 (2005) 113.
[23] G.V. Shanbhag, B.M. Devassy, S.B. Halligudi, J. Mol. Catal. A: Chem. 218 (2004) 67.
[24] M. Misono, in: L. Guszi, et al. (Eds.), Proceedings of the 10th International Congress Catalysis, Budapest, Hungary, Elsevier, Amsterdam, 1993, p. 69.
[25] T. Masuda, A. Igarashi, Y. Ogino, J. Jpn. Petrol. Inst. (1980) 30.
[26] T. Blasco, A. Corma, A. Martinez, P. Martinez-Escoano, J. Catal. 177 (1998) 306.
[27] Q.H. Xia, K. Hidajat, S. Kawi, Chem. Commun. (2000) 2231.
[28] C.L. Chen, T. Li, S. Cheng, H.P. Lin, C.J. Bhongale, C.Y. Mou, Micropor. Mesopor. Mater. 50 (2001) 201.
[29] Y. Sun, L. Zhu, H. Lu, R. Wang, S. Lin, D. Jiang, F.S. Xiao, Appl. Catal. A-Gen. 6058 (2002) 1.
[30] W. Hua, Y. Yue, Z. Gao, J. Mol. Catal. A: Chem. 170 (2001) 195.
[31] M.V. Landau, L. Titelman, L. Wradman, P. Wilson, Chem. Commun. (2003) 594.
[32] Y. Li, S.T. Wong, M.C. Chao, H.P. Lin, C.Y. Mou, S. Cheng, Appl. Catal. A-Gen. 261 (2004) 211.
[33] S. Choi, Y. Wang, Z. Nie, J. Liu, C.H.F. Peden, Catal. Today 55 (2000) 117.
[34] P.M. Rao, M.V. Landau, A. Wolfson, A.M. Shapira-Tchelet, M. Herskowitz, Micropor. Mesopor. Mater. 80 (2005) 43.
[35] A. Kawada, S. Mitamura, S. Kobayashi, Syn. Lett. 7 (1994) 545.
[36] I. Hachiya, M. Moriwaki, S. Kobayashi, Tet. Lett. 36 (1995) 409.
[37] I. Hachiya, M. Moriwaki, S. Kobayashi, Bull. Chem. Soc., Jpn. 68 (1995) 2053.
[38] K. Suzuki, M. Mukoyama, Japan Patent 06 145 092, 1994.
[39] M. Spagnol, L. Gilbert, D. Alby, Ind. Chem. Libr. 8 (1996) 29.
[40] T. Raja, A.P. Singh, A.V. Ramaswamy, A. Finiels, P. Moreau, Appl. Catal. A-Gen. 211 (2001) 31.
[41] C. Guignard, V. Pédron, F. Richard, R. Jacquat, M. Spagnol, J.M. Coustard, G. Pérot, Appl. Catal. A-Gen. 234 (2002) 79.
[42] P. Moreau, A. Finiels, P. Meric, J. Mol. Catal. A: Chem. 154 (2000) 185.
[43] B.M. Choudary, M. Sateesh, M.L. Kantam, K.V. Ram Prasad, Appl. Catal. A-Gen. 171 (1998) 155.
[44] G.D. Yadav, H.G. Manyar, Micropor. Mesopor. Mater. 63 (2003) 85.
[45] M. Hartmann, S. Racouchot, C. Bischof, Micropor. Mesopor. Mater. 27 (1999) 309.
[46] K. Schumacher, M. Grün, K. Unger, Micropor. Mesopor. Mater. 27 (1999) 201.
[47] J. He, X. Duan, C. Li, Mater. Chem. Phys. 71 (2001) 221.
[48] C. Cong-Yan, L. Hong-Xin, M.E. Davis, Micropor. Mater. 2 (1993) 17–26.
[49] R. Schmidt, M. Stöcker, M.D. Akporiaye, E.H. Tørstad, A. Olsen, Micropor. Mater. 5 (1995) 1.
[50] W. Kuang, A. Rives, M. Fournier, R. Hubaut, Appl. Catal. A-Gen. 250 (2003) 221.
[51] L. Pizzio, P. Vázquez, C. Cáceres, M. Blanco, Catal. Lett. 4 (2001) 77.
[52] A.V. Emeline, G.V. Kataeva, A.S. Litke, A.V. Rudakova, V.K. Ryabchuk, N. Serpone, Langmuir 14 (1998) 5011.
[53] M. Misono, Chem. Commun. 13 (2001) 1141.
[54] E. Lopez-Salinas, J.G. Hernandez-Corez, I. Schifter, E. Torres-Garcia, J. Navarrete, A. Gutierrez-Carillo, T. Lopez, P. Lottici, D. Bersani, Appl. Catal. A-Gen. 193 (2000) 215.
[55] N. Essayem, Y.Y. Tong1, H. Jobic, J.C. Vedrine, Appl. Catal. A-Gen. 194/195 (2000) 109.
[56] R.I. Maksimovskaya, Kinet. i Katal. 36 (1995) 836.
[57] Y. Kand, K.Y. Lee, S. Nakata, S. Asaoka, M. Misono, Chem. Lett. (1988) 139.
[58] Y. Hirano, K. Inumaru, T. Okuhara, M. Misono, Chem. Lett. (1996) 1111.
[59] S. Uchida, K. Inumaru, J.M. Dereppe, M. Misono, Chem. Lett. (1998) 643.
[60] B.H. Davis, R.A. Keogh, S. Alerasool, D.J. Zalewski, D.E. Day, P.K. Doolin, J. Catal. 183 (1999) 45.
[61] Y. Zong, X.M. Pan, L.Y. Duan, Y.C. Xie, Chin. J. Catal. 18 (1997) 321.
[62] K. Tanabe, M. Misono, Y. Ono, H. Hattori, Stud. Surf. Sci. Catal. 51 (1989) 169.
[63] Y. Nakano, T. Iizuka, H. Hattori, K. Tanabe, J. Catal. 57 (1978) 1.
[64] T. Jin, T. Yamaguchi, K. Tanabe, J. Phys. Chem. 90 (1986) 4794.
[65] J. Kaur, K. Griffin, B. Harrison, I.V. Kozhevnikov, J. Catal. 208 (2002) 448.
[66] D.G. Barton, S.L. Soled, G.D. Meitzner, G.A. Fuentes, E. Iglesia, J. Catal. 181 (1999) 57.